COBEM 2023 27TH INTERNATIONAL CONGRESS OF MECHANICAL ENGENEERING

ABCM Brazilian Society of Mechanical Sciences and Engineering
27th ABCM International Congress of Mechanical Engineering
December 04-08, 2023, Florianópolis-SC, Brazil

COB-2023-1435
EVALUATING ULTRASONIC FLOW METER PARAMETERS THROUGH COMPUTATIONAL SIMULATION OF FLOWS WITH FLOW CONDITIONER

Tulio Rafael Nascimento Porto
João Alves de Lima
Federal University of Paraíba - PPGEM/CT/UFPB & DEER/CEAR/UFPB
João Pessoa/PB, Brazil.
trnp@academico.ufpb.edu.br; jalima@cear.ufpb.br

Tony Hebert Freire de Andrade
Federal University of Campina Grande, Department of Petroleum Engineering
Campina Grande/PB, Brazil.
tonyherbert@uaepetro.ufcg.edu.br

Antonio Gilson Barbosa de Lima
Federal University of Campina Grande, Department of Mechanical Engineering
Campina Grande/PB, Brazil.
antonio.gilson@ufcg.edu.br

Abstract. *Accurate flow rate measurements play a major role in the control of several industrial processes, and the ultrasonic flow meters have stood out as the most appropriate devices for measurements of gaseous flows, mainly due to their non-intrusive properties. To try to assure the measurement's quality, sometimes unsuccessfully, these devices normally apply measurement corrections based on some characteristic flow parameters, such as asymmetry, crossflow, and swirl, which quantify deviations from the fully developed flow pattern, to which most flow meters, including the ultrasonic ones, are usually designed and which often does not consider flow disturbances caused by bends, valves and other connections used in the industrial field. In this context, to minimize flow perturbations and therefore reduce the ultrasonic flow meter effort to correct flow variations, the present work assesses, through computational fluid dynamics, the use of flow conditioners, in order to align the flow streamlines and minimize flow meter corrections based on the above-cited flow parameters. At the present research stage, the flow conditioner is positioned after two natural pipeline perturbations (two in-plane 90º bends) at a specific position (5D after the last bend), and the measurements are taken at five predefined positions relative to the last bend: one before the flow conditioner (2D), and four after it, 10D, 15D, 20D, 25D). According to the preliminary computational results, the application of the designed flow conditioner drastically enhanced the quality of the diagnostic flow parameters (reduction at the position 10D at most 2.8 times of the asymmetry deviation (from -13% to -4.5%), at most 2.7 times of the crossflow deviation (from -3.2% to -1.2%), and at most 22.5 times of the swirl deviation (from -7.7% to -0.34%)), reducing, therefore, the requirement of ultrasonic flow meter measurement corrections.*

Keywords: *Ultrasonic flow meters, flow conditioners, asymmetry, crossflow, swirl*

1. INTRODUCTION

Ultrasonic flow meters operate based on acoustic waves emitted by piezoelectric sensors, which act both as emitters and receivers of these acoustic signals. They evaluate the average flow velocity, V, of a fluid flowing inside a duct with inner diameter D, through dynamic measurements of the propagation velocity, V_{AB}, along an acoustic path (AB) of length Lp (that forms an angle ϕ with the longitudinal axis duct, normally 45º), which is a function of the transit times (t_{AB} and t_{BA}) from the pulses emitted by both sensors (A and B) (Thompson, 2011). To increase accuracy, more than one pair of acoustic sensors are employed along the duct transversal section, in predefined radial positions. Figure 1 illustrates a configuration with four pairs of transducers (a four-path ultrasonic flow meter: paths AB, CD, EF, and GH).

$$V_{AB} = \frac{L_p}{2\cos\phi}\left(\frac{1}{t_{AB}} - \frac{1}{t_{BA}}\right) \tag{1}$$

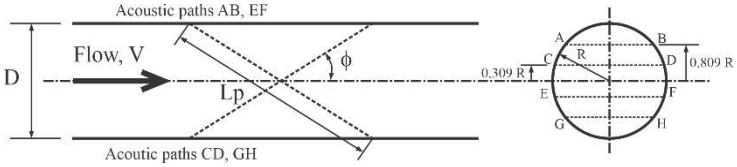

Figure 1. A four-pair-sensors ultrasonic flow meter configuration

The average flow velocity V (and therefore the flow rate) inside the duct is evaluated through numerical integration (Gaussian quadrature) across the duct transversal cross-section (Seiler,2016):

$$V = \sum_{i=1}^{N} w_i V_i \tag{2}$$

Where i stands for the i-th acoustic path, so V_i is the i-th acoustic path average velocity and w_i is the i-th associated quadrature weight.

The accuracy of the ultrasonic flow meter will be greater the closer to the developed region it is located since less correction should be applied by the sensors. Regarding turbulent flow in rectilinear ducts, the hydrodynamic flow length varies between 25 and 80 hydraulic diameters. This ideal design condition is impracticable in most situations due to space limitations often found in industrial applications, where the pipeline system is often constituted by geometric accidents such as bends and section reductions that promote flow perturbations mainly when placed upstream of the flow meters (Grimley, 1997; Grimley, 2002; Martins and Ramos, 2011; Martins et al., 2021; Drenthen et al., 2009).

The impacts of perturbations in flow field are normally measured by the asymmetry, crossflow, and swirl parameters. Asymmetry is obtained as the ratio between the mean velocities in the acoustic paths in the upper half (AB and CD) to the mean velocities in the lower half of the channel (EF and GH). This parameter quantifies the deviation of the maximum velocity profile from the duct centerline. Crossflow is characterized by the appearance of two vortices of opposite rotations in the duct cross-section, often caused by a bend in the pipeline. It is obtained by the ratio between the mean velocities along two dissimilar perpendicular acoustic paths, AB-EF and CD-GH. In its turn, swirl characterizes flows that developing in a spiral fashion. Normally, such a flow condition appears when two bends in distinct planes are present in the pipeline. This parameter is also called the flow profile factor, which relates the mean velocities in the outer acoustic paths (AB and GH) with the mean velocities in the inner acoustic paths (CD and EF). In fully-developed flows, asymmetry, and crossflow must have the unit value, while swirl must attain the value 1.17 (Zanker, 2010; Zhao et al., 2014).

$$\text{Asymmetry} = \frac{V_{AB} + V_{CD}}{V_{EF} + V_{GH}} \tag{3}$$

$$CrossFlow = \frac{V_{AB} + V_{EF}}{V_{CD} + V_{GH}} \tag{4}$$

$$Swirl = \frac{V_{CD} + V_{EF}}{V_{AB} + V_{GH}} \tag{5}$$

The effects of flow disturbances can extend up to 200 diameters (200D), which makes the application of flow meters in practical engineering cases very restricted, although modern ultrasonic flow meters bring internal algorithms that try to correct the measured flow rate based on the above-mentioned flow parameters. To increase the robustness of the measurement devices, it is normally introduced flow conditioners that enable the alignment of flow streamlines, in order to minimize the flow disturbances that reduce the quality of the measurement parameters or reduce the length of straight pipe required to accurately measure the flow rate (Zhao et al., 2014).

Therefore, the present work aims at assessing the use of flow conditioners in a duct that is employed to evaluate flow meters through computational fluid dynamics (CFD), demonstrating the improvement of the main flow metric parameters (asymmetry, crossflow, and swirl) often used in ultrasonic flow meters.

2. PROBLEM DESCRIPTION

We study the flow behavior of air at ambient temperature (T_{amb} = 300 K, density $\rho = 1.225\ \text{kg/m}^3$and dynamic viscosity $\mu = 1.7894\times10^{-5}$ kg/m.s) inside a circular duct with inner diameter D = 198.17 mm and two 90 degree in-plane

bends, as depicted in Figure 2. Air enters the duct with uniform velocity u_{in} = 4.282 m/s and leaves it at null relative pressure.

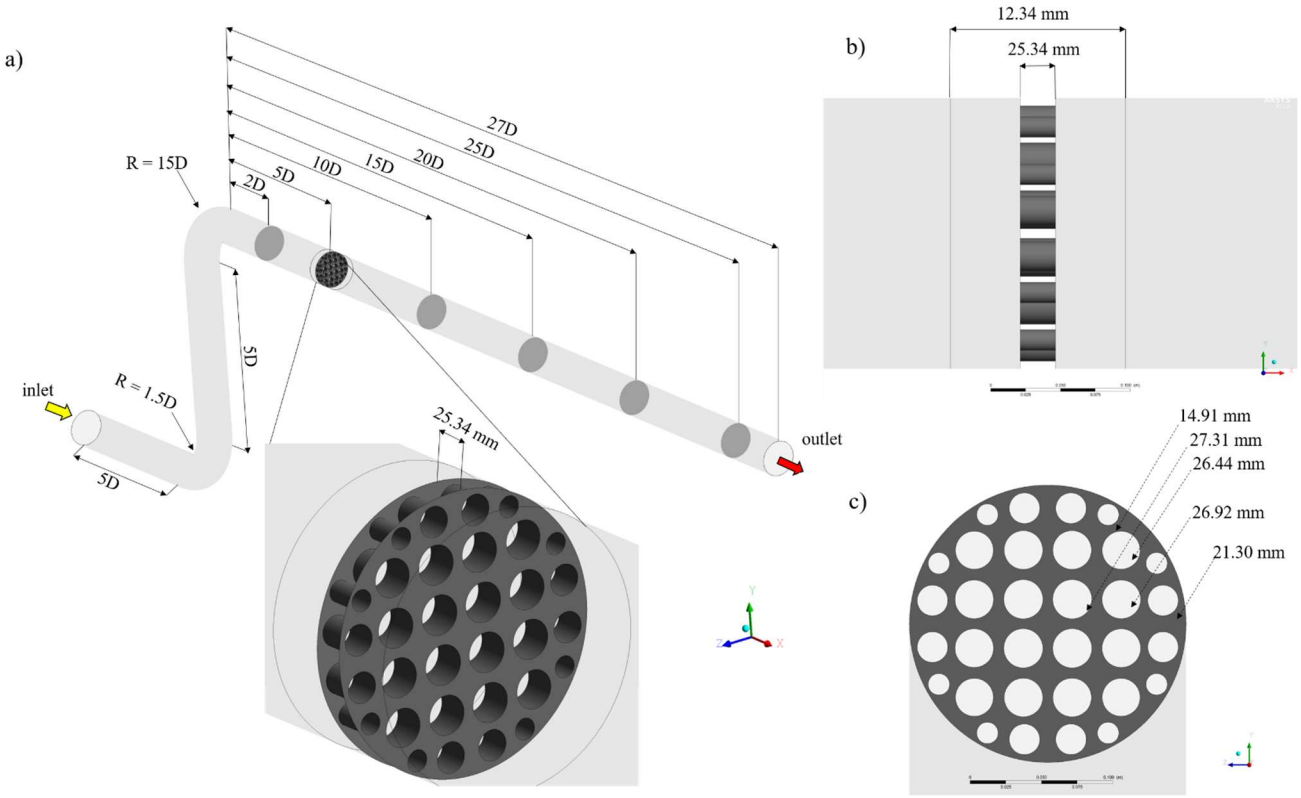

Figure 2. Flow geometry: a) isometric view of the duct with the locations of the measurements stations, and flow conditioner in detail, b) flow conditioner lateral view; c) flow conditioner frontal view.

Five reference planes were employed at positions 2D, 10D, 15D, 20D and 25D downstream the second duct bend to verify the flow behavior (velocity and pressure profiles) and evaluate the diagnostic flow metrics (asymmetry, crossflow, and swirl), with and without a flow conditioner (a 32-orifice plate of varied hollow diameters with thickness of 25.34 mm, as illustrated in Figure 2).

3. MATHEMATICAL MODELLING AND SOLUTION

The governing equations for the flow field description are given by the incompressible form of the mass conservation equation, the Navier-Stokes equations and the equations of the turbulence model adopted (here, the k-ω SST model was selected for predicting the turbulence behavior (Menter,1994; Wilcox,1998). The system of equations and boundary conditions was discretized and solved through the Ansys FLUENT® software (Ansys Inc, 2015), which is based on the finite volume method (Patankar, 1980; Versteeg and Malalasekera, 2007). The applied boundary conditions are the standard inlet (uniform velocity, u_{in} = 4.282 m/s, medium turbulence level), outlet (zero relative pressure) and non-slip wall.

Regarding the numerical mesh, for the situation with no flow conditioner, it was employed a mesh with 1,304,000 elements, while for the situation with flow conditioner, a more refined mesh with 5,000,000 elements was required to achieve an acceptable convergence tolerance. Figure 3 illustrates a typical mesh and its particularities according to the flow regions (bends, transition regions, and flow conditioner region).

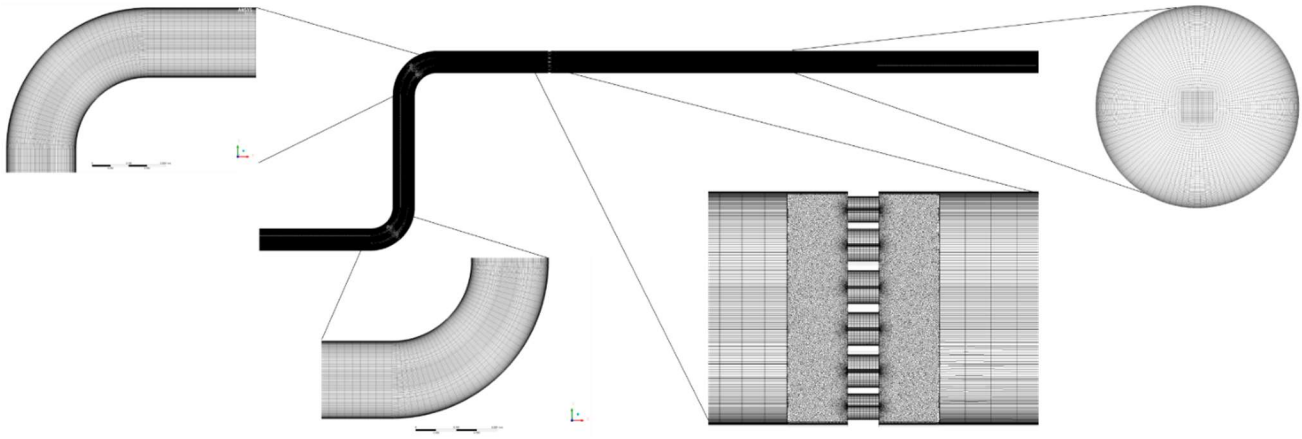

Figure 3. Details of the typical meshes employed in the simulations illustrating the bend, transition and flow conditioner mesh regions.

As one can see, to accommodate the large variations in geometric scales between the main pipe and the flow conditioner, two mesh-transition regions were inserted, bounded at 50mm before and after the flow conditioner. In these regions, meshes were constructed with polyhedral elements in the inner part of the pipe and with refined hexahedral layers near the wall. In the other regions of the pipe, hexahedral elements were applied through a partition technique that suits the cylindrical pipe geometry, in addition to the use of more refined layers near the wall (to adequately capture the strong velocity gradients).

4. RESULTS AND DISCUSSION

Figures 4a and 4b illustrate a comparison of the longitudinal velocity component profile along the five selected transversal planes with and without the use of the flow conditioner. These profiles are drawn in a line that splits in half the transversal section, in a xy-plane at position z = 0.

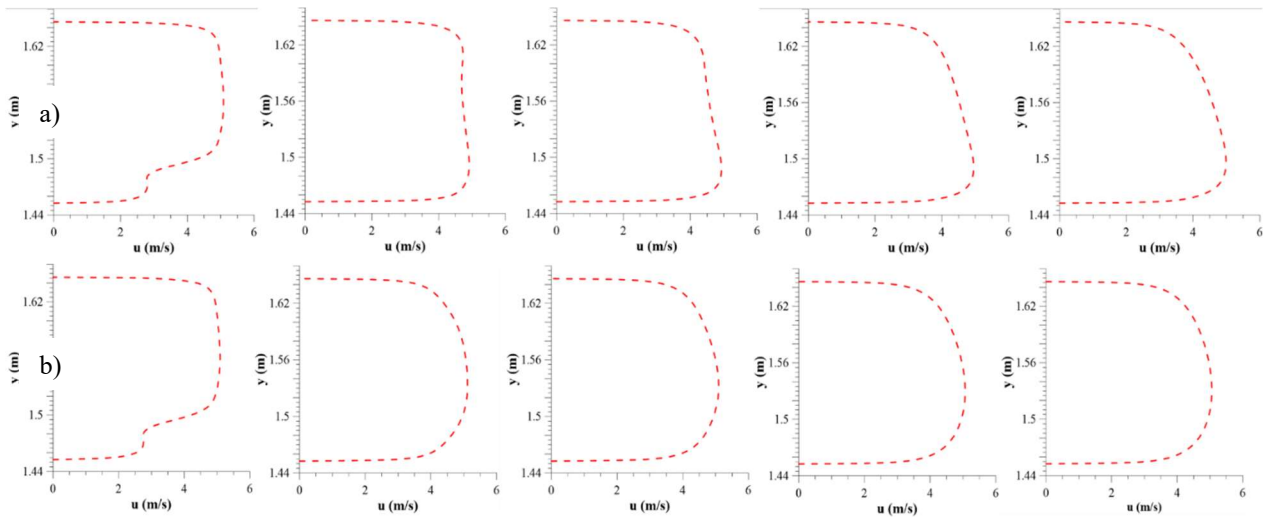

Figure 4. Velocity profiles at five selected duct transversal positions: a) no flow conditioner, b) with flow conditioner.

The Figure 4a shows, that for the plane positioned at 2D, the velocity profiles accelerated towards the upper half of the duct, with velocities reaching values almost twice that found in the lower half part. This effect is rebated towards the bottom part after position 10D when the velocity reaches almost 5 m/s. Figure 4b demonstrates the efficacy of the flow conditioner since the velocity field now exhibits a velocity profile approximately symmetric. The fluid acceleration at the lower half part of the duct can also be observed in Figure 5 through the curvature in the streamlines after the second duct bend, and in Figure 6, through the velocity vectors in the same planes, according to the velocity range.

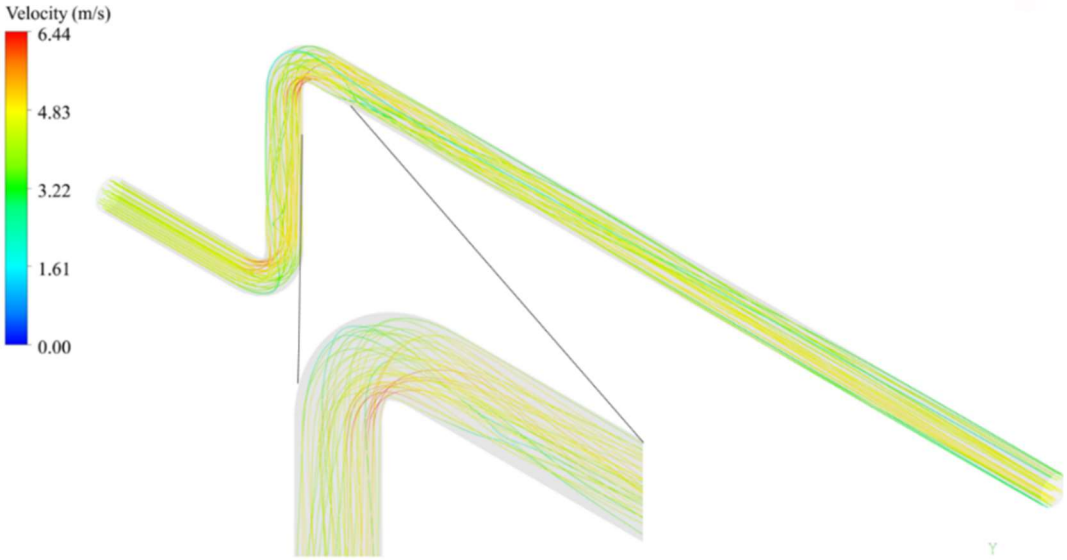

Figure 5. Curvature of the flow streamlines in a region near de duct bend. Duct with no flow conditioner.

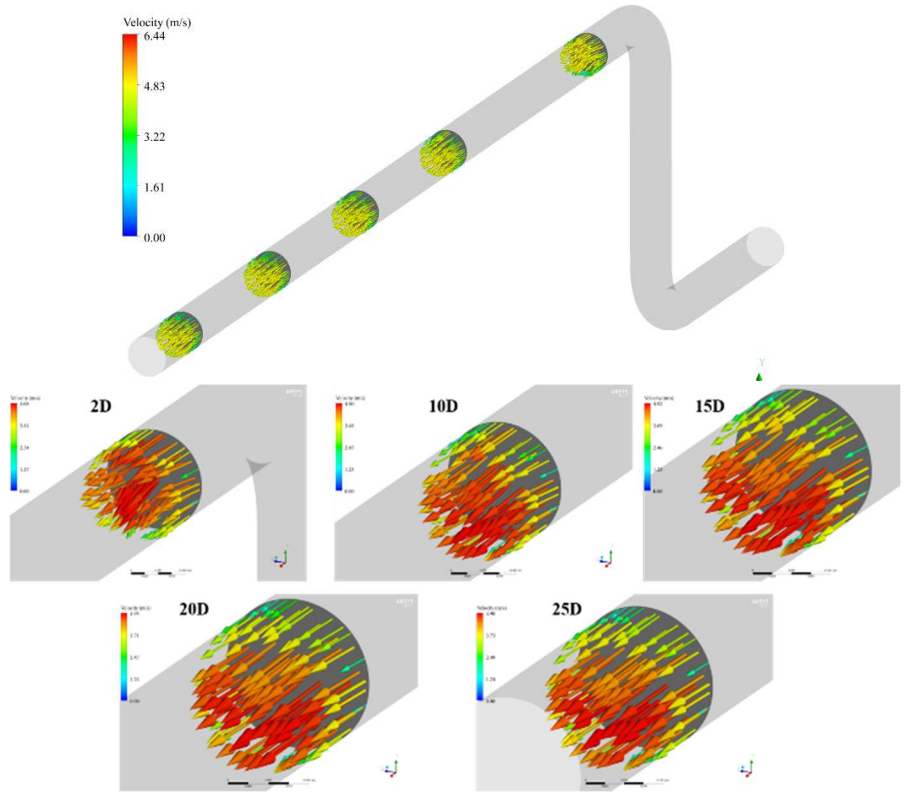

Figure 6. Velocity vectors at the five selected transversal planes: a) global velocity scale, b) local velocity scale. Duct with no flow conditioner.

Figure 6 also reveals that the acceleration of the fluid towards the lower half part of the duct is maintained along the duct for several lengths after the perturbations, effect that is drastically reduced with the implementation of a flow conditioner, as it is observed in Figs. 7 and 8, which illustrate the flow streamlines for the situation with flow conditioner. As observed, despite of the flow homogenization, the velocity (and the pressure drop) magnitude are greatly increased, since fluid is forced to flow in a smaller area.

Figure 9 brings the velocity vectors for the duct with flow conditioner in the same transversal planes illustrated in Figure 6 and, additionally, in the flow conditioner region. The flow adjustment for symmetry is notably markable and indicates that the diagnostic flow parameters certainly will be improved when using a flow conditioner.

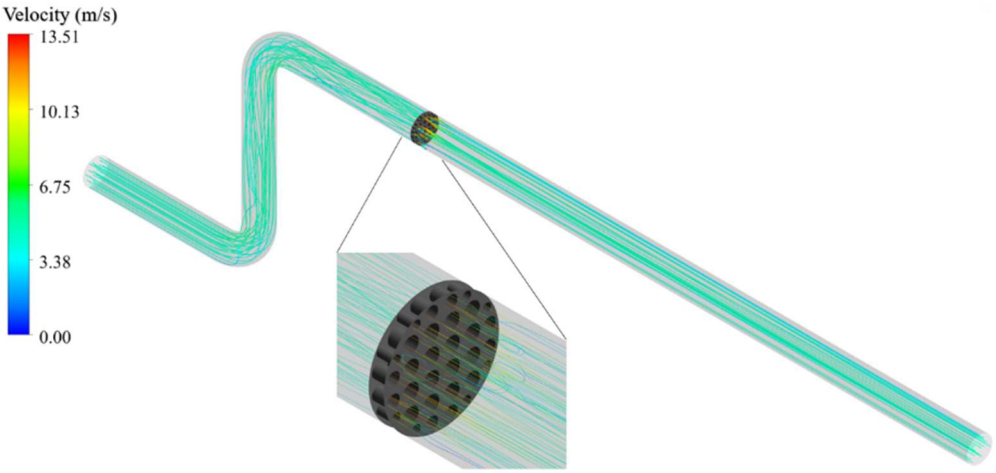

Figure 7. Isometric view of the flow streamlines along the duct and near the flow conditioner (in detail).

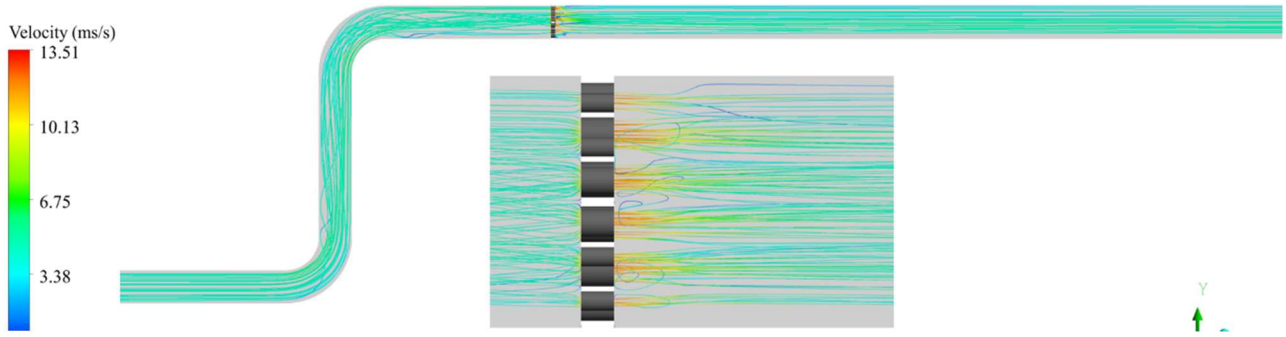

Figure 8. Lateral view of the flow streamlines along the duct and near the flow conditioner (in detail) in a *xy*-plane at z = 0.

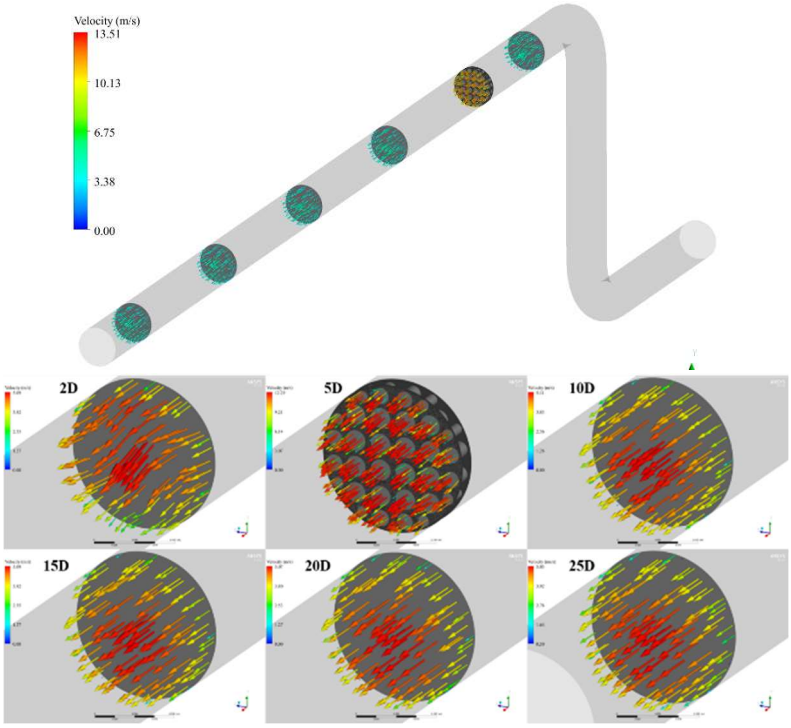

Figure 9. Velocity vectors at selected transversal planes: a) global velocity scale, b) local velocity scale. Duct with flow conditioner.

According to Figure 9, it is observed that all velocity vectors are almost aligned at position x = 10D, although a slight concentration of vectors with higher velocity intensities in the lower half of the duct is still observable.

For better visualization and discussion, Figs. 10 and 11 bring velocity contours at the five selected transversal planes along the duct, for the situations where the flow conditioner is not applied and where it is employed, respectively.

A comparison between these figures shows the marked effect of flow homogenization when using a flow conditioner. Figure 10 shows that without the flow conditioner, to achieve a fully developed flow condition several prohibitive duct lengths will be required, showing that the asymmetry caused by the duct bend is very strong. On the other hand, for the situation with flow conditioner, Figure 11 clearly shows that after x = 10 D the flow field can be considered almost symmetric. Although the flow field is not completely symmetric, the effort of the ultrasonic flow meter to provide a more accurate measurement will certainly be reduced, improving its accuracy.

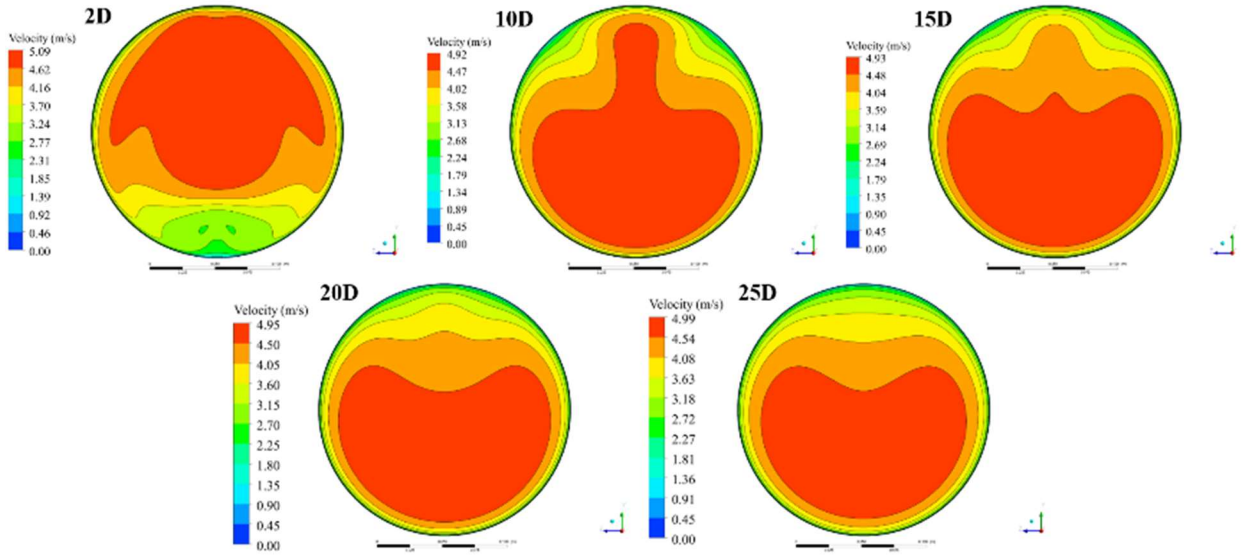

Figure 10 – Velocity contours at the five selected transversal planes along the duct. Case with no flow conditioner.

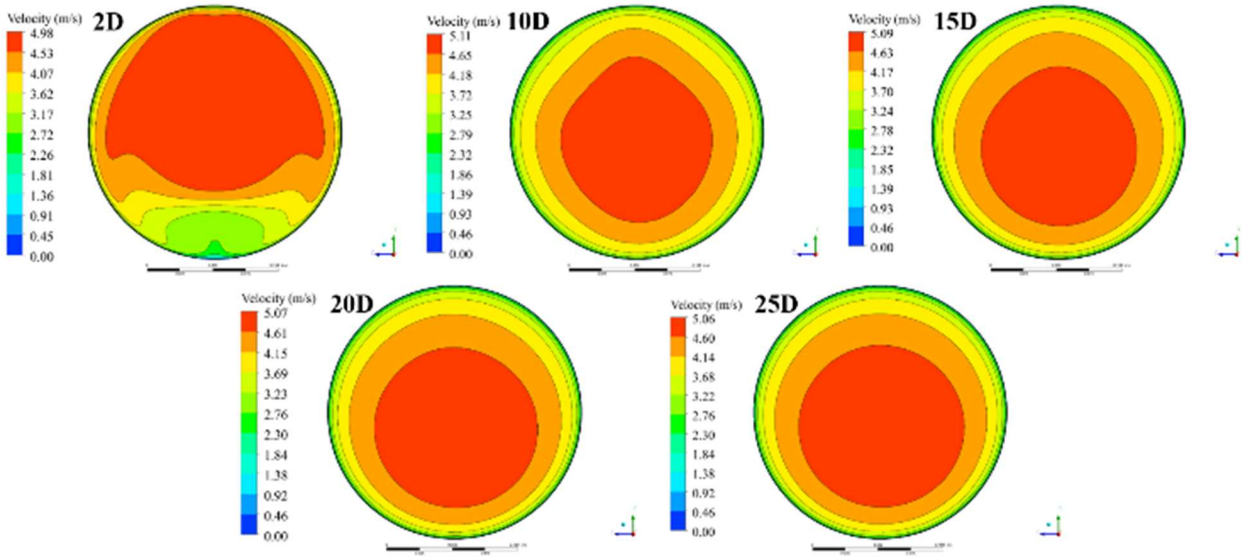

Figure 11 – Velocity contours at the five selected transversal planes along the duct. Case with a flow conditioner.

To quantify the flow behavior with and without a flow conditioner, Table 1 brings the values of the three diagnostic flow parameters evaluated in the five selected transversal sections, demonstrating the positive influence of the flow conditioner on these ultrasonic flow meter metrics.

Table 1: Flow diagnostic parameters values and their relative deviations in relation to the fully developed flow.

x position	Asymmetry		Crossflow		Swirl	
	No Flow Conditioner	Flow Conditioner	No Flow Conditioner	Flow Conditioner	No Flow Conditioner	Flow Conditioner
2D	1.227 (23%)	1.221 (22%)	1.194 (19%)	1.194 (19%)	1.228 (5.0%)	1.215 (3.8%)
10D	0.874 (-13%)	0.955 (-4.5%)	0.968 (-3.2%)	0.988 (-1.2%)	1.080 (-7.7%)	1.166 (-0.34%)
15D	0.836 (-16%)	0.936 (-6.4%)	0.920 (-8.0%)	0.982 (-1.8%)	1.148 (-1.9%)	1.167 (-0.26%)
20D	0.834 (-17%)	0.932 (-6.8%)	0.912 (-8.8%)	0.978 (-2.8%)	1.185 (1.3%)	1.175 (0.43%)
25D	0.842 (-16%)	0.938 (-6.2%)	0.922 (-7.8%)	0.980 (-2.0%)	1.202 (2.7%)	1.179 (0.77%)
∞	1.000		1.000		1.170	

As can be seen from this table, for the transversal section positioned in x = 2D, values of the diagnostic parameter asymmetry are very distant from that expected for the fully developed flow (1.000), with or without the flow conditioner (1.221 and 1.227, respectively). This demonstrates that inserting the flow conditioner at the position in x = 5D will not alter significantly the upstream flow, however, at the downstream of the flow conditioner, for example at x = 10D, the flow conditioner tries to make the flow field symmetric (asymmetry from 0.874 to 0.955, a reduction of at most 2.8 times on the difference in relation to the fully developed unity value).

Table 1 also reveals that for this kind of flow perturbations (two in-plane bends), crossflow and swirl are almost not present in the flow development (at the position x = 10D, crossflow (0.968 and 0.988) is close to unity and swirl (1.080 and 1.166) is close to 1.170), phenomena that are expected when analyzing flow perturbation in more than one plane (two out-plane bends, for example). Notwithstanding, at this position, crossflow and swirl differences values are reduced at most 2.7 times and 22.5 times, respectively, in relation to the fully developed values, when using the flow conditioner.

5. CONCLUSIONS

The present work demonstrated that computational fluid dynamics can be employed to study and design optimized flow conditioners that impact the flow field characteristics and the quality of the diagnostic parameters employed in ultrasonic flow meters (asymmetry, crossflow, and swirl). Despite an increase in the pressure drop, the proposed flow conditioner was able to align the flow field for the operational conditions studied, reducing flow distortions and improving the ultrasonic flow meter diagnostic parameters. Simulations with more general flow perturbations (out-plane bends), the design of optimized flow conditioners for several flow operational conditions, and optimal positioning of the flow conditioner are in current progress.

6. REFERENCES

Ansys Inc., Ansys Fluent Theory Guide, Release 15.07, 2015.

D.C. Wilcox, “Turbulence Modeling for CFD”, DCW Industries, La Canada, CA, 1998.

D. Seiler, “Fundamentals of Multipath Ultrasonic Flow Meters for Liquid Measurement”, 2016. [Online]. Available: http://asgmt.com/wp-content/uploads/2016/02/061_.pdf.

E. Thompson, “Fundamentals of multipath ultrasonic flow meters for gas measurement”. American School of Gas Measurement Technology, 2011. [Online]. Available: https://asgmt.com/wp-content/uploads/pdf-docs/2011/1/F05.pdf.

F.R. Menter, “Two-equation eddy-viscosity turbulence models for engineering applications”. AIAA Journal, vol. 32, n. 8, 1994, pp. 1598-1605.

H. Zhao, L. Peng, S.A. Stephane, H. I., K. Shimizu, M. Takamoto, “CFD Aided Investigation of Multipath Ultrasonic Gas Flow Meter Performance Under Complex Flow Profile”, IEEE Sensors Journal, vol. 14, n. 3, March 2014.

H. Versteeg, W. Malalasekera, An Introduction to Computational Fluid Dynamics: The Finite Volume Method, Pearson, 2nd edition, February, 2007.

J. G. Drenthen, M. Kurth and M. Vermeulen. “Verification of ultrasonic gas flow meter”. CEESSI Ultrasonic Seminar, Jun. 2009, pp. 1-16.

K.J. Zanker, “Diagnostic Ability of the Daniel Four Path Ultrasonic Flow Meter”, Daniel Measurement and Control White Papers, Daniel Industries, USA, 2010, pp. 1-8.

R.S. Martins and R. Ramos, “Bend installation effects on the correction factor of single path ultrasonic flow meters. In: Proceedings of XXXII Iberian Latin American Congress on Computational Methods in Engineering, 2011, p. 579-587.

R.S. Martins, G.S. de Aquino, M.F. Martins, R. Ramos, "Sensitivity analysis for numerical simulations of disturbed flows aiming ultrasonic flow measurement", Measurement, vol. 185, 110015, 2021.
S.V. Patankar, Numerical Heat Transfer and Fluid Flow, New York, Hemisphere, 1980.
T.A. Grimley, "Performance testing ultrasonic flow meters", North Sea Flow Measurement Workshop, Paper 19, Kristiansand, Norway, October 1997.
T.A. Grimley, "Metering Research Facility Program: Performance Testing of 12-Inch Ultrasonic Flow Meters and Flow Conditioners in Short Run Meter Installations", draft topical report (Jan. 1999–June 2000) to Gas Research Institute, Report No. GRI-01/0129, GRI Contract No. 5097-170-3937, February 2002, Des Plaines, IL.

7. RESPONSIBILITY NOTICE

The authors are the only responsible for the printed material included in this paper.